metals

MDPI

Article

Fatigue Performance Evaluation of K-Type Joints in Long-Span Steel Truss Arch Bridge

Peng Liu [1], Hongping Lu [1], Yixuan Chen [1], Jian Zhao [2], Luming An [2] and Yuanqing Wang [3,*]

[1] School of Architecture and Civil Engineering, Shenyang University of Technology, Shenyang 110870, China
[2] China Railway Construction Bridge Engineering Bureau Group Co., Ltd., Tianjin 300300, China
[3] Department of Civil Engineering, Tsinghua University, Beijing 100084, China
* Correspondence: wang-yq@mail.tsinghua.edu.cn

Abstract: The K-type joint, which consists of the web members and the chord members with varied angles welded together, has been widely adopted in long-span steel truss bridges. However, its fatigue performance has been rarely considered, despite its critical role in bridge structural safety and durability. Accordingly, the FE model of the K-type joint was established in Abaqus and the fatigue performance analysis was conducted, in which the effect of web/chord thickness ratio (τ), chord/web angle (θ), and chord with rib stiffener were investigated. Take the Mingzhu Bay steel truss arch bridge as an engineering background, the hot spot stress method was employed to calculate the fatigue performance of three K-type joints in unfavorable locations. Furthermore, a 3D full-scall bridge model was built to evaluate the fatigue performance of the K-type joints under standard and overloaded moving vehicle load scenarios. The results show that the max hot spot stress factor (SCF_{max}) of the web and chord member is influenced by τ and θ. The chord members added stiffener is founded to be an effective way to enhance fatigue performance. The fatigue stress intensities of the three unfavorable locations meet the Eurocode 3 specification requirements, but the one in the mid-truss arch is not satisfied under an overloaded vehicle loading rate of 25%.

Keywords: K-type joint; fatigue performance; hot spot stress; finite element analysis; steel truss arch bridge

Citation: Liu, P.; Lu, H.; Chen, Y.; Zhao, J.; An, L.; Wang, Y. Fatigue Performance Evaluation of K-Type Joints in Long-Span Steel Truss Arch Bridge. *Metals* **2022**, *12*, 1700. https://doi.org/10.3390/met12101700

Academic Editor: Marino Brčić

Received: 20 September 2022
Accepted: 10 October 2022
Published: 11 October 2022

1. Introduction

The K-type joints have been widely used in long-span steel truss arch bridges. It comprises the chord members, and web members welded together to transit the deck system load, moving vehicle load and wind load to the lower arch ribs. These K-type joints are subject to dynamic vehicle loading with repeated cyclic stress amplitude. Due to the light weight of steel truss bridge, the internal stress generated from the moving vehicle load accounts for a large portion of total stress in the K-type joints. Hence, the welded joint of steel truss bridges is prone to fatigue failure [1]. Moreover, the stress distribution at the welded intersection is complex and stress concentration often occurs which endangers the durability and safety of the bridge. Such as the Seongsu bridge on the Han River in South Korea suddenly collapsed in 1994, the main reasons reported were the welding quality and overloading condition that triggered the fatigue crack failure of the steel truss joint and led to a collapse accident. Also, the I-35W bridge on the Mississippi river suddenly collapsed in 2007, it was found that I-35W had serious joint corrosion and fatigue cracking, but little attention has been paid, which eventually led to the collapse during 40 years in service. The bridge collapse photos are shown in Figure 1.

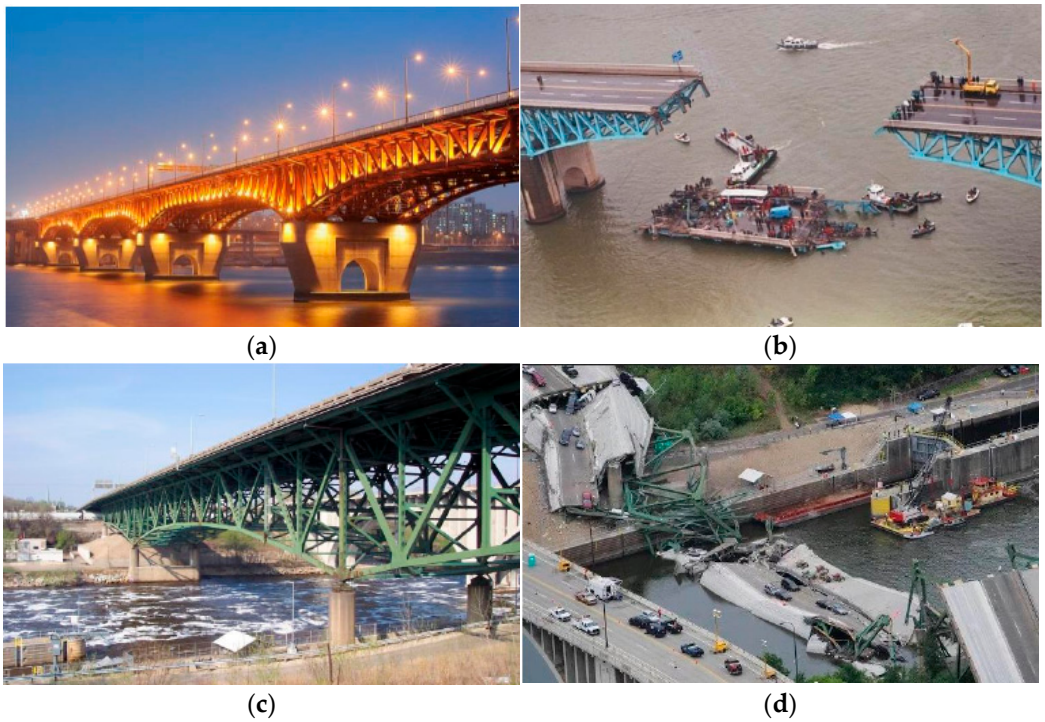

Figure 1. The Bridge collapse accident [2]. (**a**) The Seongsu Bridge in service; (**b**) Collapse of the Seongsu Bridge; (**c**) The I-35W Bridge; (**d**) Collapse of the I-35W Bridge.

For steel bridge welding fatigue failure, many research activities are fulfilled in past decades. In 2007, Sturm et al. [3] proposed a method to determine the allowable initial size of welding defects, which is a function of the required fatigue strength of the weld. The effects of the main parameters are discussed quantitatively, and design suggestions are proposed. In 2012, Aygül et al. [4] selected five different welded joints commonly used in steel bridges to study the accuracy and applicability of the fatigue assessment methods. The evaluation results of each method are compared with the recommended fatigue strength values in Eurocode 3 [5] and International Welding Association (IIW) specification [6]. The results show that although the nominal stress method is simple, it can still obtain satisfactory results. In 2016, Baptista et al. [7] re-calculated the existing fatigue detailed design suggestions and conduct four different types of CHS pipes under high cycle conditions. The results were calculated by the local notch stress method and compared with the previous fatigue tests in the literature. In 2017, Cai et al. [8] studied the applicability of the effective notch stress method on large-scale T-joints of truss bridges through numerical analysis. The results show that the effective notch stress method provides a conservative estimate of fatigue strength. In 2018, Alencar et al. [9] used the hot spot stress method (HSM) to evaluate the fatigue life of welded joints affected by deformation-induced fatigue, considering the progressive deterioration model of the vehicle speed and pavement. In 2020, Shin [10] calculated the cross-shaped fillet weld with full penetration and incomplete penetration by three-dimensional fatigue finite element analysis and carried out load-bearing and non-load-bearing analysis. The results show that local stress is very important to evaluate the fatigue performance of existing road bridges. In 2021, Yang [11] et al. studied the fatigue performance of load-carrying fillet-welded (LCFW) cross joints, including fatigue strength, S-N curve, crack shape, fatigue crack growth rate, and fatigue life prediction method. In 2021, Alencar et al. [12] further extended the reference verification by using the available fatigue strength data of large-scale tests on typical bridge structure details. The method is adopted as the basis for establishing the current nominal S-N curves available in American specifications. In 2022, Luo et al. [13] investigated the fatigue performance of the slit end region where the slotted circular hollow section (CHS) pipe is connected with the gusset plate. Wang et al. [14] evaluated the

reliability of the effective notch stress (ENS) method recommended by IIW and proposed appropriate modification parameters. Jie et al. [15] carried out tensile fatigue tests on cracked cross joints strengthened with carbon fiber reinforced polymer. The results show the effect of welding speed on residual stress is greater than that of welding current and a better reinforcement by carbon fiber reinforced polymer.

Also of concern of several experimental and numerical studies are on the wedded joints in steel bridges. In 2012, Guo et al. [16] proposed a probabilistic finite element analysis method in combination with the traffic load model to evaluate the time-varying fatigue reliability level of steel bridge welding details. In 2017, Liu et al. [17] used the fatigue load model to evaluate the fatigue life, the results show that the connection between the truss and the beam at the transition point is prone to fatigue damage. In 2018, Yuan et al. [18] used a probabilistic finite element model to estimate the microscopic small fatigue crack growth in the weld of bridge steel. The simulation is based on a microstructure sensitive crystal plasticity model, which is used to quantify the fatigue index parameter (FIP) at the level of the slip system, and a fatigue model that correlates FIP with the fatigue life of a single grain. In 2018, K. R. et al. [19] studied the applicability and appropriateness of the C-S criterion based on the critical plane method in fatigue damage assessment of welded joints of railway steel bridges. In 2020, Mashayekhi et al. [20] proposed a fatigue assessment scheme for these complex key components of steel bridges using the hot spot stress method. A computational efficient finite element model of large bridges is established to provide local structural responses of complex components under dynamic traffic loads. In 2022, Horas et al. [21] proposed a comprehensive fatigue analysis method for existing metal railway bridges, and gradually implemented fatigue assessment methods. Yuan et al. [22] proposed a fatigue damage evolution model based on damage mechanics to evaluate the fatigue damage of steel bridge welded joints. Skoglund et al. [23] studied and compared the fatigue strength of four different structural detail solutions through numerical simulation. Compared with the traditional solutions currently used, the structural details can improve fatigue strength by more than 25%.

In summary, although many studies have been conducted on the fatigue performance of the welded joint, the fatigue performance of the K-type joints in long-span steel truss bridges has been rarely considered. This paper studies the effect of web/chord thickness ratio (τ), chord/web angle (θ), and chord with stiffener on the fatigue performance of the K-joint of steel truss arch bridge. Take the Mingzhu Bay steel truss arch bridge as the engineering background, the hot spot stress method was employed to calculate the fatigue performance of three unfavorable locations. Furthermore, a 3D full-scall bridge model was built to evaluate the fatigue performance of the K-type joints under standard and overloaded moving vehicle load scenarios.

2. Method

2.1. K-Type Joint

The K-type joint adopts Q420qD steel, and its chemical composition is shown in Table 1. The welding process is conducted in the factory. The welding method is penetration welding and the parameters are shown in Table 2. The welding sequence takes the way of inside welding first and then outside welding. The gas used for gas welding is CO_2, the welding wire is E501T-1L, the diameter is 1.2 mm. The outer submerged arc welding adopts plate element boat type submerged arc welding, the welding material is H08MnA wire, the diameter is 5 mm, and the flux is SJ101q.

Table 1. Chemical Composition of Q420qD.

Chemical Composition	C	Si	Mn	P	S	Nb	V	Ti	Cr	Ni	Cu	N	Mo
Mass fraction/%, ≤	0.20	0.50	1.70	0.035	0.035	0.07	0.20	0.20	0.30	0.80	0.30	0.015	0.20

Table 2. Welding parameters of penetration welding.

Welding Position	Welding Material	Welding Current/A	Voltage/V	Welding Speed/(cm/min)
Vertical welding	E501T-1L(Φ1.2 mm) +CO_2	140–180	24–26	40
Flat welding	H08MnA(Φ5 mm) +SJ101q	220–280	24–26	40

The K-type joint was used as a load transit component in the steel truss bridge structure. Based on the Mingzhu Bay Bridge, the finite element model of the K-type joint was established in Abaqus, and three hot spot positions were selected as focus points, as shown in Figure 2. A 20-node reduced integral solid element (C3D20R) was used for simulation and the bottom chord of the K-typed joint is fixed.

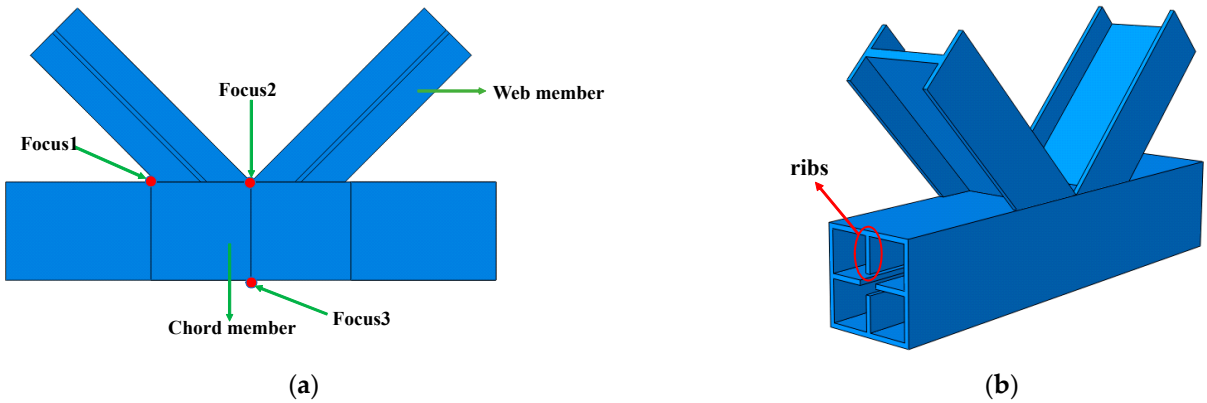

Figure 2. FE model of the K-type joint. (**a**) Focus points; (**b**) With rib stiffener.

2.2. Modeling and Parameters

Table 3 lists the FE model parameters design on fatigue performance. To investigate the effect of the geometric parameters of K-type welded joints on the stress concentration coefficient, the angle between the chord and web member θ, the thickness ratio of web member to chord member τ, and chord member with/without stiffener was selected to conduct the parametric analysis in Abaqus. Herein, a total of 13 finite element models are established for analysis, the parameters commonly used in truss bridges: 30 °≤ θ ≤60°, 0.25≤ τ ≤ 1.0.

Table 3. FE model of the K-type welded joints.

FE Model No.	Parameters		Chord with Stiffener
	θ	τ	
1	30°	0.25	×
2	30°	0.5	×
3	30°	0.75	×
4	30°	1	×
5	45°	0.25	×
6	45°	0.5	×
7	45°	0.75	×
8	45°	1	×
9	60°	0.25	×
10	60°	0.5	×
11	60°	0.75	×
12	60°	1	×
13	60°	0.5	√

In a steel truss bridge structure, the K-type joint could carry the axial load, bending moment, or both together. In order to calculate the stress of K-type joints more accurately, the load of joints is decomposed into three basic load conditions according to technical specification [24], as shown in Figure 3.

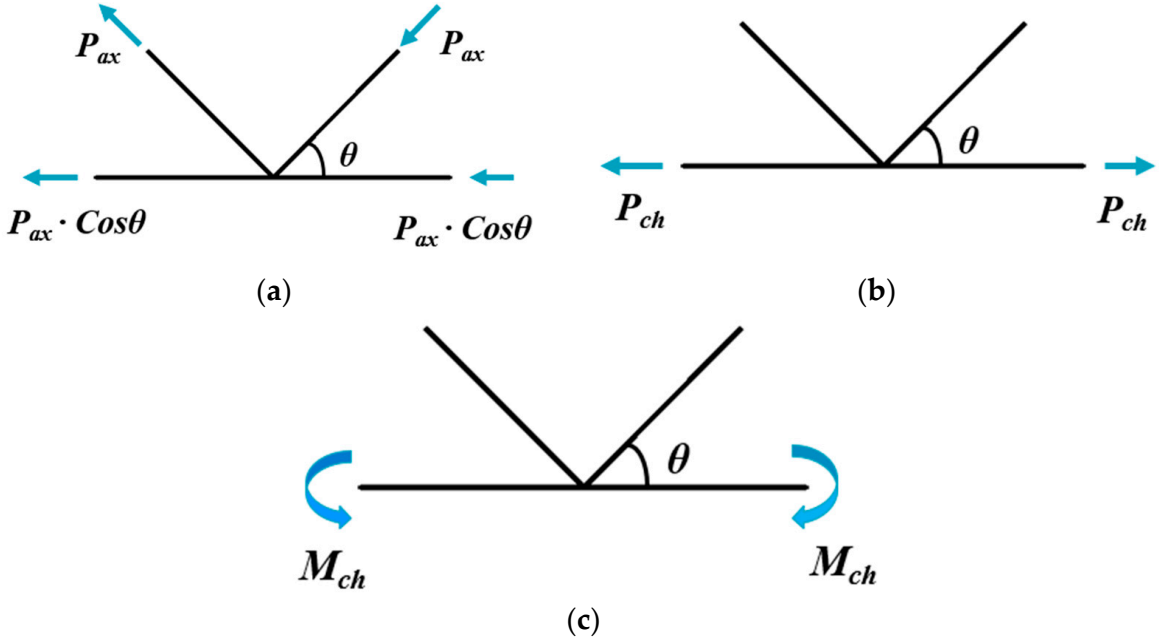

Figure 3. Three basic load conditions of K-type welded joints. (**a**) Axial force in chord and web member; (**b**) Axial force in chord member; (**c**) Bending moment load in chord member.

2.3. Maximum Hot Spot Stress Factor

Hot spot stress refers to the maximum stress of the structure or the stress of the dangerous point of the component. The structural stress is calculated by the finite element method or simple mechanical formula according to the loading condition. The welded size and defects is not considered.

The stress concentration factor (SCF) is defined as the ratio of hot spot stress to nominal stress under a certain basic load condition. The distribution of SCF along the perimeter of the joint is varied, but there are several positions where the maximum value of SCF may occur, which are determined as hot spots. The hot spot stress at each structural detail is obtained by the linear extrapolation method recommended by the IIW specification [6]. The calculation equation of SCF parameters of K-type joints is given below [25]:

Load case I (Axial force in chord and web member):

$$SCF_{max} = \left(0.48\beta - 0.5\beta^2 - \frac{0.12}{\beta} + 0.012/g'\right) \cdot (2\gamma)^{1.72} \cdot \tau^{0.78} \cdot g^{0.2} \cdot (\sin\theta)^{209} \quad (1)$$

Load case II (Axial force in chord member only) and Load case III (Bending moment in chord member only):

$$SCF_{max} = (2.45 + 1.23\beta) \cdot g^{-0.27} \quad (2)$$

where β is the width ratio of the chord to web member, and 2γ is the width-to-thickness ratio of the chord, in bridge engineering, gap joints g ($g > 0$) is recommended, and the ratio of gap and weld thickness is defined as dimensionless parameter g'.

2.3.1. Influence of Thickness Ratio τ on SCF_{max}

The effect of the thickness ratio τ on SCF_{max} of the K-type joint under three basic load cases is shown in Figure 4. The values plotted in the figure were obtained from FE model analysis. According to Equations (1) and (2), the SCF_{max} of the K-joint is calculated.

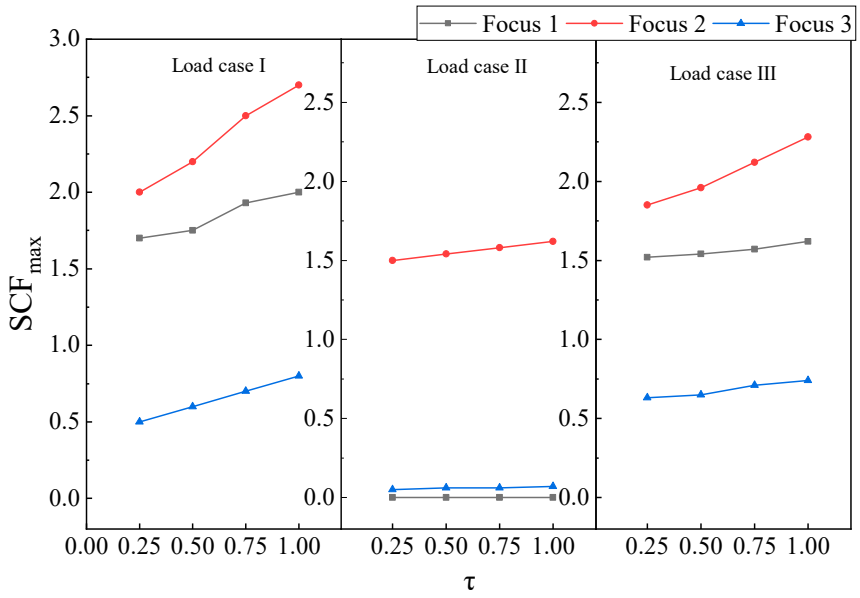

Figure 4. The effect of τ on SCF_{max} (θ = 45°).

It can be seen from Figure 4 that under load case 1, SCF_{max} on chords and webs and τ It is positively correlated, while for load cases 2 and 3, SCF_{max} is not sensitive to τ. This is because with the increase of web thickness, the uneven stiffness distribution at the section of concern 1 becomes more serious, leading to the increase of SCFmax.

2.3.2. Influence of Angle θ on SCF_{max}

Based on the FE model analysis and Equations (1) and (2), the effect of the thickness ratio θ on SCF_{max} of the K-type joint under three basic load cases is shown in Figure 5.

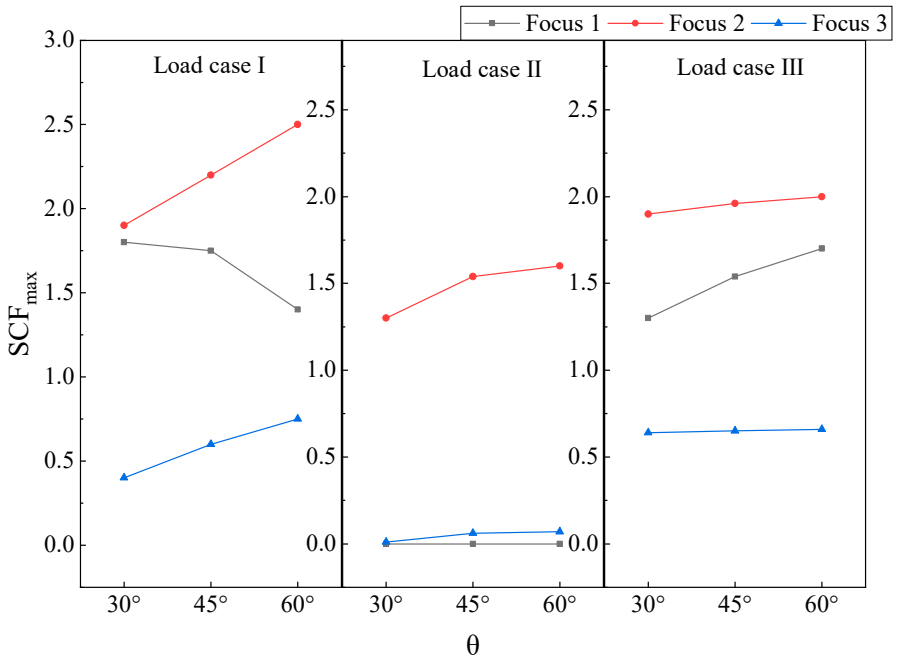

Figure 5. Effect of θ on SCF_{max} (τ = 0.5).

It can be seen from Figure 5, the SCF_{max} and θ are almost positively correlated and increase in a linear relationship, except for focus 2 when the θ is larger than 45°. Indeed, the angle between the chord and web is suggested to be smaller than 45° to benefit the fatigue performance of K-joints.

2.3.3. Influence of Rib Stiffener on SCF_{max}

Assume the thickness ratio of the web member to the chord member is 0.5 and the angle is 45°, the SCF_{max} of K-joint can be obtained from FE model analysis and Equations (1) and (2). Figure 6 shows the influence of the rib stiffener on SCF_{max} under three basic load cases.

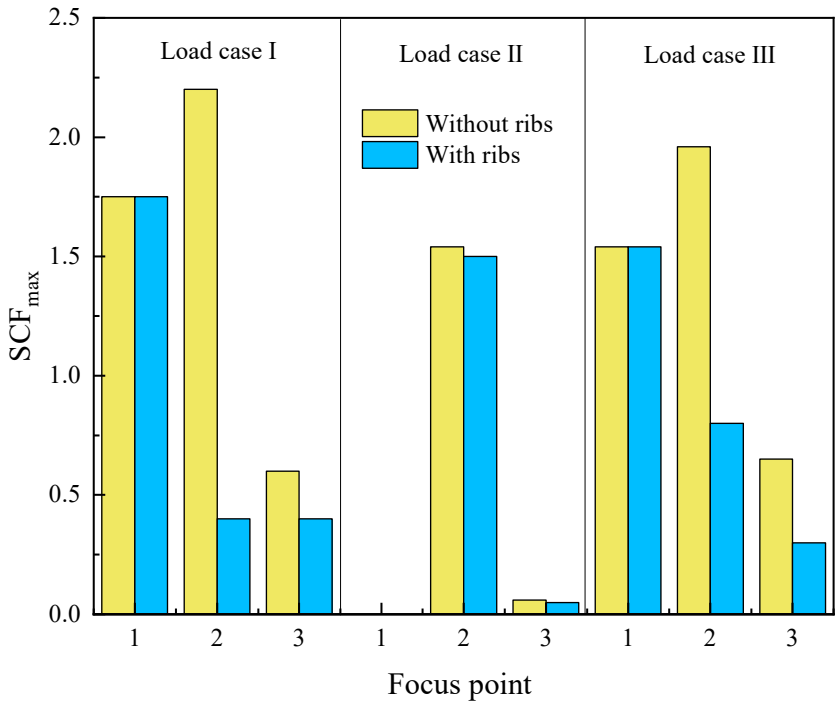

Figure 6. Effect of chord rib on SCF_{max} ($\tau = 0.5$, $\theta = 45°$).

It can be seen from Figure 6, the SCF_{max} of the K-joints with rib stiffeners are all smaller than others in any load case, which indicates the fatigue performance is enhanced by rib stiffener. Therefore, the rib stiffener of the K-joints is encouraged in an actual steel truss bridge.

3. Case Study: The Mingzhu Bay Bridge

3.1. Project Overview

The main bridge of Mingzhu Bay is 96 m + 164 m + 436 m + 164 m + 96 m + 60 m long, with three main steel truss arches, with a total length of 1016 m; The double deck layout is adopted. The upper layer is a two-way eight lanes highway, and the sidewalks are on each side. The total width of the deck is 43.2 m, On both sides of the lower layer are four lanes reserved for the city lines [26,27]. The K-type joints of the main truss structure are made of Q420qD steel. The bridge elevation is shown in Figure 7.

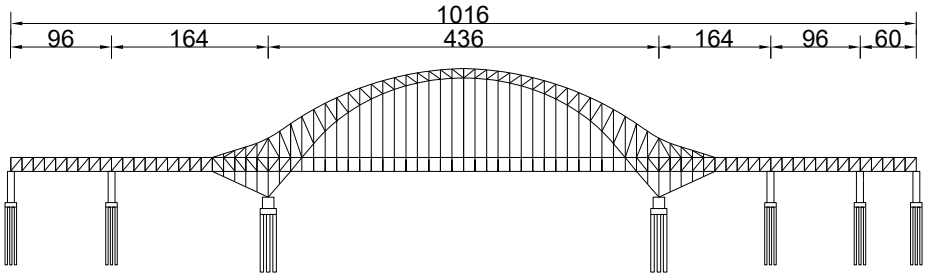

Figure 7. Elevation of the Mingzhu Bay bridge (Unit: m).

3.2. 3D finite Element Model

The 3D full-scall bridge model was established by Midas finite element software to conduct fatigue analysis. The spatial beam element is used to simulate the structure of arch rib, steel truss and pier. The consolidation of arch foot is used as the boundary condition. The pier is rigidly connected with T-beam and cover beam of deck, and the welded joints are rigidly connected. The conditions of dead load and second-stage pavement load are defined. The moving load conditions are defined according to the highway grade and lane layout.

According to preliminary analysis, the fatigue-vulnerable joints of the bridge are located as A, B, and C, and the focus points of each K-type joint are labeled as a, b, and c, shown in Figure 8.

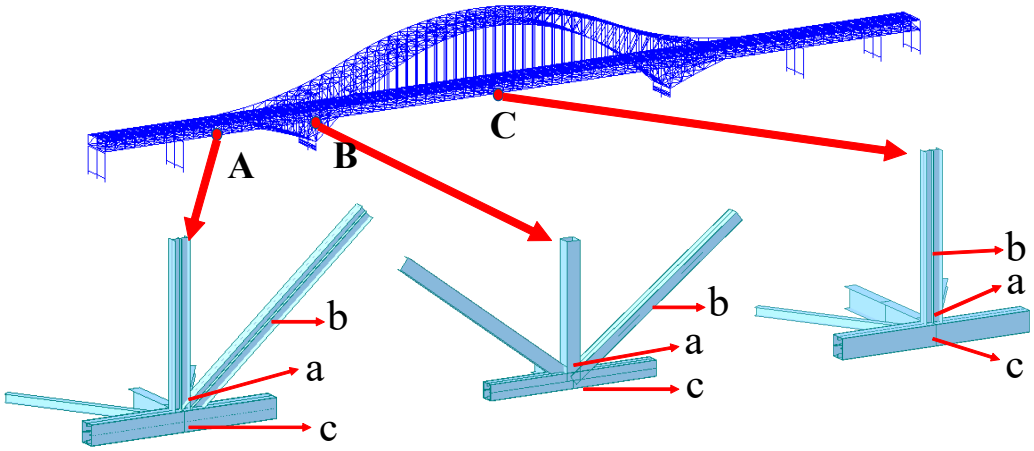

Figure 8. FE model of the Mingzhu Bay Bridge.

3.3. Hot Spot Stress Amplitude

Based on the vehicle flow statics [28], the moving vehicle load was divided into seven fatigue vehicle models to load on the FE model [29]. At bridge locations of A, B, and C, the nominal stress of K-type joints labeled as a, b, and c were obtained from the results of the FE bridge model. Moreover, with the corresponding SCF_{max} mentioned in 2.3, the hot spot stress amplitude is shown in Figure 9.

As shown in Figure 9, despite the stress varied as moving vehicles load for the joint location A, the stress amplitude is small, which is around 30 MPa. However, the stress amplitude of the K-type joint near the steel truss arch support vibrates larger than the other positions at joint location B. For the joint location C, the curve is smooth, while the peak stress is not over 60 MPa.

3.4. Fatigue Performance Analysis

3.4.1. Standard Vehicle Load

In Eurocode [5], the fatigue resistance of bridge welded joints can be evaluated according to the following equation:

$$\gamma_{Ff}\Delta\sigma_{E,2} \leq \frac{\Delta\sigma_C}{\gamma_{Mf}} \quad (3)$$

where γ_{Ff} is 1.35, $\Delta\sigma_{E,2}$ is hot spot stress amplitude. Based on the S-N (Figure 10) curve of the fatigue strength of the hot spot stress method, $\Delta\sigma_C$ is 92 MPa, 90 MPa, and 93 MPa respectively., and the calculation results of the maximum hot spot stress amplitude are shown in Table 4.

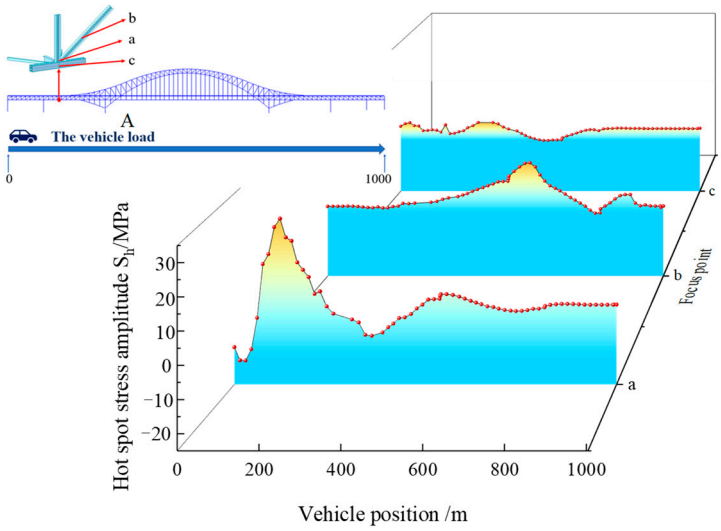

(**a**)

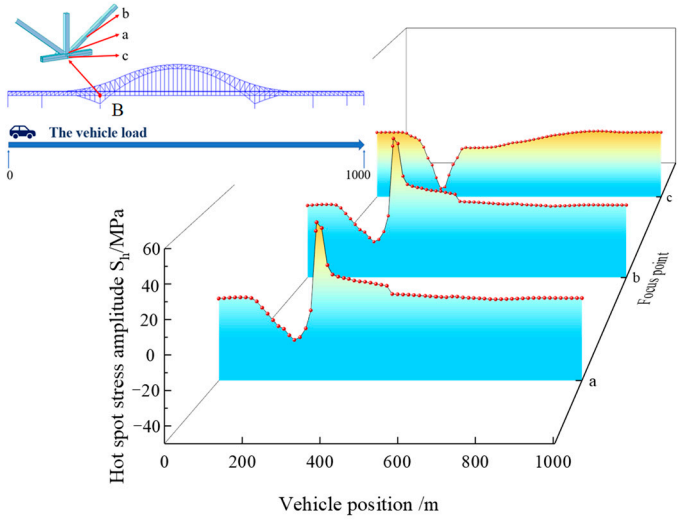

(**b**)

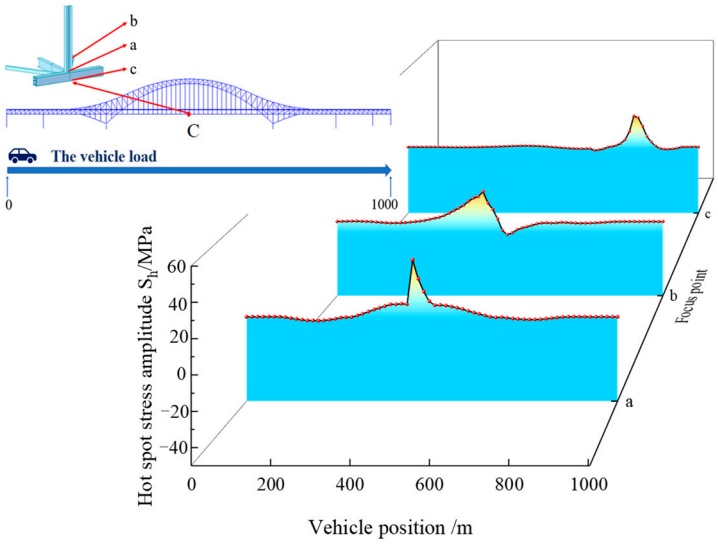

(**c**)

Figure 9. Stress response of K-type joints under moving vehicle load. (**a**) location A; (**b**) location B; (**c**) location C.

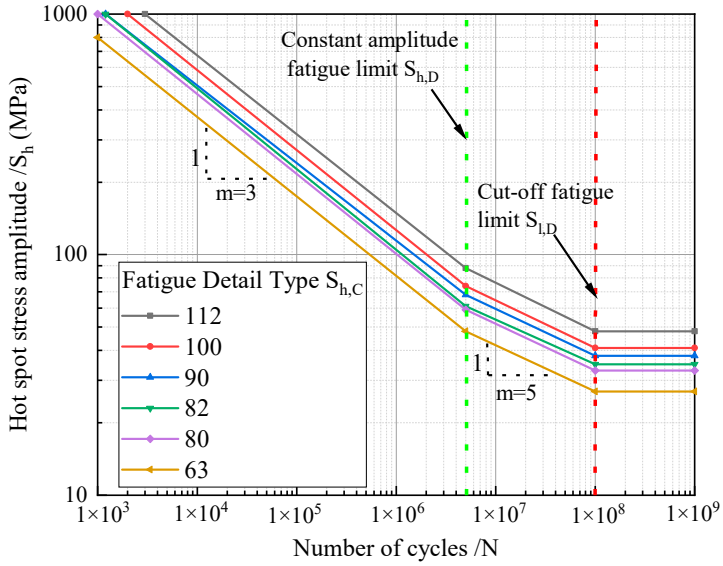

Figure 10. Fatigue strength S-N curve for each structural detail.

Table 4. Maximum Hot Spot Stress Amplitude of the Mingzhu Bay Bridge joint.

Joint No.	Focus Points on K-Type Joints					
	a		b		c	
	Calculation /MPa	Eurocode 3 /MPa	Calculation /MPa	Eurocode 3 /MPa	Calculation /MPa	Eurocode 3 /MPa
A	27.12	68.15	15.40	68.15	4.70	68.15
B	46.00	66.67	45.90	66.67	43.40	66.67
C	33.64	68.89	20.11	68.89	23.40	68.89

From Table 4 the maximum hot spot stress amplitude of the K-type joints are less than Eurocode, which meets the fatigue design requirements.

3.4.2. Overloaded Vehicle Load

The moving vehicle overload rate of 25% and 50% were considered and the results are shown in Figure 11.

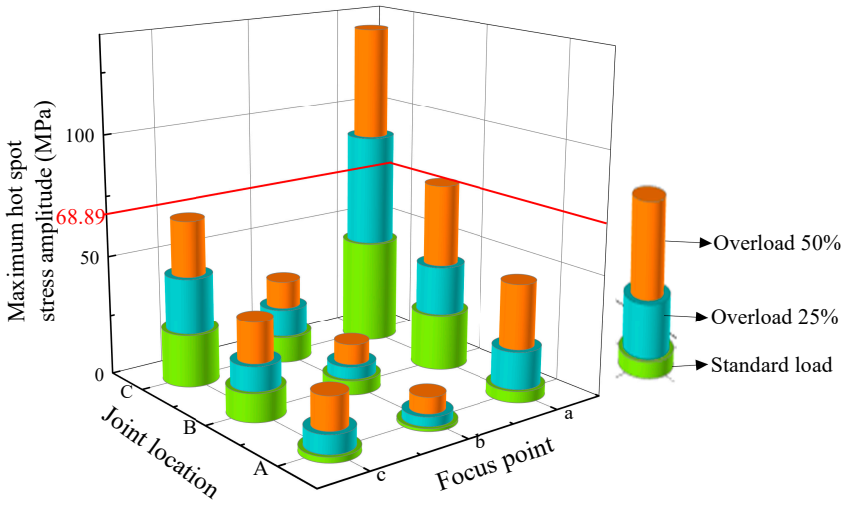

Figure 11. Maximum hot spot stress amplitude of K-type joints under overloading.

The max hot stress limit is 68.89 MPa in the Eurocode. As shown in Figure 11, the K-type joint location C, in which near the steel truss arch support and the focus point a, which is the welding area of the web member and chord of the joint is sensitive to overloading rate. Indeed, under the action of 25% overload, the maximum hot spot stress amplitude at the welding position of the web member and chord (which is labeled as 'a') is greater than 68.89 MPa, which does not meet the Eurocode 3.

4. Conclusions

This paper studied the fatigue performance of the K-type joints in the long-span steel truss bridge, providing parametric and case studies in the process. The conclusions outlined below were drawn:

1. The effect of parameters τ, θ, and rib stiffener on SCF_{max} were discussed. For K-type joints under axial force load in chord and web member, SCF_{max} is positively correlated with τ and θ, while under axial force and bending moment in chord member, thickness ratio τ and angle θ have a slight impact on SCF_{max}. Adding rib stiffener is the most effective way to enhance the fatigue performance of the K-type joints.
2. The K-type joints of the Mingzhu Bay steel truss arch bridge were calculated as a case study. With standard vehicle load, the SCF_{max} of the K-type joint is near the arch support and the web and chord welded seam is found to be the vulnerable fatigue failure area, but the hot spot stress meets the Eurocode 3 specification.
3. The overload rate of 25% and 50% were considered to investigate the fatigue performance of the K-type joint. With an overload rate of 25%, the hot spot stress in the welded seam of the chord and web member is over 68.89 MPa, which does not meet Eurocode 3 specifications.

Author Contributions: P.L., H.L. and Y.C. wrote the manuscript together; J.Z. and L.A. conducted data processing and drawings; Y.W. revised the manuscript. All authors have read and agreed to the published version of the manuscript.

Funding: Science and Technology Research and Development Project of China Railway Construction Bridge Engineering Bureau Group Co., LTD. (DQJ-2018-A01), Tianjin Science and Technology Development Plan Project (19YDLZSF00030).

Institutional Review Board Statement: Not applicable.

Informed Consent Statement: Not applicable.

Data Availability Statement: Not applicable.

Acknowledgments: The authors would like to thank China Railway Construction Bridge Engineering Bureau Group Co., Ltd. for the test data and funding support.

Conflicts of Interest: The authors declare no conflict of interest.

References

1. Shi, W.H.; Zhong, X.G. Study on stress concentration coefficient of K-shaped tubular joints under axial load. *Eng. Mech.* **2010**, *27*, 48–52.
2. Long, X. Evaluation and comparison of fatigue structural details of welded joints of steel truss bridges based on hot spot stress method. PhD Thesis, Chang'an University, Xi'an, China, 2021.
3. Haldimann-Sturm, S.C.; Nussbaumer, A. Fatigue design of cast steel nodes in tubular bridge structures. *Fatigue* **2008**, 528–537. [CrossRef]
4. Aygül, M.; Bokesjö, M.; Heshmati, M.; Al-Emrani, M. A comparative study of different fatigue failure assessments of welded bridge details. *Int. J. Fatigue* **2013**, *49*, 62–72. [CrossRef]
5. *EN 1993-1-9*; Eurocode 3: Design of steel structures—Part 1–9: Fatigue. European Committee for Standardization: Bruxelles, Belgium, 2005.
6. Zhao, X.-L.; Packer, J.A. IIW Document XIII-1804-99 and IIW Document XV-1035-99: Recommendations of IIW Subcommission XV-E. In *Fatigue Design Procedure for Welded Hollow Section Joints*; Abington Publishing: Cambridge, UK, 2000; ISBN 978-1-85573-522-4.
7. Baptista, C.; Kannuna, S.; Pedro, J.O.; Nussbaumer, A. Fatigue behavior of CHS tubular bracings in steel bridges. *Int. J. Fatigue* **2017**, *96*, 127–141. [CrossRef]

8. Cai, S.; Chen, W.; Kashani, M.M.; Vardanega, P.J.; Taylor, C.A. Fatigue life assessment of large scale T-jointed steel truss bridge components. *J. Constr. Steel Res.* **2017**, *133*, 499–509. [CrossRef]
9. Alencar, G.; de Jesus, A.M.; Calçada, R.A.; da Silva, J.G.S. Fatigue life evaluation of a composite steel-concrete roadway bridge through the hot-spot stress method considering progressive pavement deterioration. *Eng. Struct.* **2018**, *166*, 46–61. [CrossRef]
10. Shin, W.; Chang, K.H.; Muzaffer, S. Fatigue analysis of cruciform welded joint with weld penetration defects. *Eng. Fail. Anal.* **2021**, *120*, 105111. [CrossRef]
11. Peng, Y.; Dai, Z.; Chen, J.; Ju, X.; Dong, J. Fatigue behaviour of load-carrying fillet-welded cruciform joints of austenitic stainless steel. *J. Constr. Steel. Res.* **2021**, *184*, 106798. [CrossRef]
12. Alencar, G.; de Jesus, A.; da Silva, J.G.S.; Calçada, R. A finite element post-processor for fatigue assessment of welded structures based on the Master S-N curve method. *Int. J. Fatigue* **2021**, *153*, 106482. [CrossRef]
13. Luo, Y.; Qiu, K.; He, M.; Ma, R.; Fincato, R.; Tsutsumi, S. Fatigue performance of the slit end area of slotted CHS tube-to-gusset plate connection. *Thin Wall Struct.* **2022**, *173*, 108920. [CrossRef]
14. Qiudong, W.; Libin, W.; Bohai, J.; Zhongqiu, F. Modified effective notch stress method for fatigue evaluation of rib-deck welds integrating the critical distance approach. *J. Constr. Steel Res.* **2022**, *196*, 107373. [CrossRef]
15. Zhiyu, J.; Kainan, W.; Shidong, L. Residual stress influence on fatigue crack propagation of CFRP strengthened welded joints. *J. Constr. Steel Res.* **2022**, *196*, 107443.
16. Tong, G.; Frangopol, D.M.; Yuwen, C. Fatigue reliability assessment of steel bridge details integrating weigh-in-motion data and probabilistic finite element analysis. *Comput. Struct.* **2012**, *112*, 245–257.
17. Liu, Z.; Hebdon, M.H.; Correia, J.A.F.O.; Carvalho, H.; Vilela, P.; De Jesus AM, P.; Calçada, R.A.B. Fatigue Life Evaluation of Critical Details of the Hercílio Luz Suspension Bridge. *Procedia Struct. Integr.* **2017**, *5*, 1027–1034. [CrossRef]
18. Hao, Y.; Wei, Z.; Castelluccio, G.M.; Jeongho, K.; Yongming, L. Microstructure-sensitive estimation of small fatigue crack growth in bridge steel welds. *Int. J. Fatigue* **2018**, *112*, 183–197.
19. Praveen, K.R.; Mishra, S.S.; Babu, P.; Spagnoli, A.; Carpinteri, A. Multiaxial Fatigue Damage Assessment of Welded Connections in Railway Steel Bridge using Critical Plane Approach. *Procedia Eng.* **2018**, *213*, 776–787.
20. Mashayekhi, M.; Santini-Bell, E. Fatigue assessment of a complex welded steel bridge connection utilizing a three-dimensional multi-scale finite element model and hotspot stress method. *Eng. Struct.* **2020**, *214*, 110624. [CrossRef]
21. Horas, C.S.; De Jesus, A.M.; Calçada, R. Efficient progressive global-local fatigue assessment methodology for existing metallic railway bridges. *J. Constr. Steel Res.* **2022**, *196*, 107431. [CrossRef]
22. Yuan, D.; Cui, C.; Zhang, Q.; Li, Z.; Zhongtao, y. Fatigue damage evaluation of welded joints in steel bridge based on meso-damage machanics. *Int. J. Fatigue* **2022**, *161*, 106898. [CrossRef]
23. Skoglund, O.; Leander, J. A numerical evaluation of new structural details for an improved fatigue strength of steel bridges. *Int. J. Fatigue* **2022**, *160*, 106866. [CrossRef]
24. *Technical Specification for Fatigue of Welded Joints of Reinforced Concrete Bridges*; DB51/T2515-2018; Sichuan Provincial Bureau of Quality and Technical Supervision: Sichuan, China, 2018. (In Chinese)
25. Zhao, X.-L.; CIDECT. *Design Guide for Circular and Rectangular Hollow Section Welded Joints under Fatigue Loading*; Design Guide No.8; TÜV-Verlag: Cologne, Germany, 2000.
26. Hu, H.; Zhao, J.; Ren, Y.; An, L.; Liu, Y. Overall design of main bridge of Guangzhou Pearl Bay Bridge. *Bridge Constr.* **2021**, *51*, 93–99. (In Chinese)
27. Zhao, J.; Yin, G.; an, L.; Liu, Y.; Ren, Y. Mid span closure technology of main bridge of Guangzhou Pearl Bay Bridge. *Bridge Constr.* **2021**, *51*, 127–133. (In Chinese)
28. Hu, H.Y.; Zhao, J.; Ren, Y.L.; An, L.M.; Liu, Y.T. Overall Design of Main Bridge of Guangzhou Mingzhu Wan Bridge. *Bridge Constr.* **2021**, *51*, 93–99. (In Chinese)
29. Liu, P.; Lu, H.; Chen, Y.; Zhao, J.; An, L.; Wang, Y.; Liu, J. Fatigue Analysis of Long-Span Steel T russ Arched Bridge Part II: Fatigue Life Assessment of Suspenders Subjected to Dynamic Overloaded Moving Vehicles. *Metals* **2020**, *6*, 1035.